Rev.Adv.Mater.Sci. 10 (2005) 437-441

DEFORMATION BEHAVIOUR OF NANOCRYSTALLINE Mg STUDIED AT ELEVATED TEMPERATURES

Z. Trojanová, P. Lukáč and Z. Száraz

Department of Metal Physics, Faculty Mathematics and Physics, Charles University, Prague, Ke Karlovu 5, CZ-121 16 Praha 2, Czech Republic

Received: May 30, 2005

Abstract. Nanocrystalline Mg samples were prepared by milling procedure in an inert atmosphere and subsequent compacted and hot extruded. The linear grain size of specimens used was estimated by X-ray line profile analysis to be about 100 nm. Compression testing was performed at temperatures from room temperature up to 300 °C. Rapid decrease of the yield stress as well as the maximum stress with temperature was observed. This decrease and the flat character of the stress strain curves at elevated temperatures indicate possible contribution of diffusion process/es and grain boundary sliding. Stress relaxation tests were conducted in order to analyse thermally activated processes occurring during plastic deformation.

1. INTRODUCTION

Magnesium, the lightest structural metallic element, and its alloys possess a great potential to be developed as structural materials provided that significant improvements in properties are achieved. Coarse grained Mg materials have some limitations such as low strength, low ductility and poor corrosion resistance. According to the Hall–Petch relationship [1,2], it can be shown that grain size refinement is the most effective method for improving the strength of materials. It is important to mention here that with grain size refinement, ductility has also been found to increase [3]. Several papers [3-7] have reported that high ductility and even low-temperature superplasticity may be obtained by grain size refinement of magnesium or magnesium alloys.

Nanocrystalline materials are characterised by small grain size, typically in the range 1-100 nm. Ultrafine grained materials exhibit the grain size 100-500 nm.

Deformation mechanisms of nanocrystalline (nc) metallic materials have been studied experimentally using mechanical testing [8-12] as well as theoretically using simulation models [13-15]. Grain boundary sliding has been found as a significant deformation process. A direct observation of grain boundary sliding at room temperature was also made using high resolution TEM by in-situ straining of nc Au. TEM images revealed large rotations and sliding between individual grains during plastic deformation to high strains with no apparent evidence of dislocation activity [8,16]. Some authors reported, in line with grain boundary sliding, deformation mechanism

Corresponding author: Z. Trojanova, e-mail: ztrojan@met.mff.cuni.cz

controlled by diffusional creep with a threshold stress as well as deformation mechanism controlled by dislocation motion. [17,18]. Compressive deformation of nc Mg (with the grain size of 42-45 nm) was studied by Hwang and co-workers [19]. They found that the main deformation mechanism operating during straining at room temperature is grain boundary sliding with the threshold stress.

In this paper, the measurements of stress strain rate curves of nanocrystalline magnesium at temperatures between 23 and 300 °C using compressive monotonic tests and stress relaxation tests are reported in order to determine its deformation mechanism.

2. EXPERIMENTAL PROCEDURE

Nc Mg samples were prepared by ball milling procedure in an inert atmosphere and subsequent consolidation and hot extrusion. The linear grain size of specimens used was estimated by X-ray line profile analysis to be about 100 nm. Uniaxial compression tests were carried out at temperatures between room temperature and 300 °C using an INSTRON testing machine. Cylindrical specimens with the diameter of 10 mm and length of 15 mm were deformed with an initial strain rate of $2.8 \cdot 10^{-4}$ s^{-1}. The temperature in the furnace was kept with an accuracy of ±1 °C. Stress relaxations (SR) for 300 s during the deformation were performed.

3. RESULTS AND DISCUSSION

Fig. 1 shows the true stress-true strain curves obtained in compression for various temperatures. Samples were deformed either to fracture or at higher temperatures to predetermined strains. Pronounced upper yield point followed by the hardening stage was observed on curves obtained at temperatures between room temperature and 100 °C. After the initial peak, the curve is once again close to being flat. The curves measured at temperatures higher than 100 °C have a steady state character, without hardening. The temperature dependences of the characteristic stresses, the yield stress σ_{02} as well as the maximum stress σ_{max}, are shown in Fig. 2. Both stresses decrease rapidly with increasing temperature.

In the case when the material was prepared by milling, the refinement of the originally large grains into the nc regime is achieved through the accumulation and rearrangement of dislocations generated during milling. This large plastic deformation is partially recovered during consolidation of the powder and subsequent hot extrusion. Such nc metals usually contain a high density of dislocations in a heavy-deformation microstructure. Internal friction measurements performed at the same material showed an internal friction peak at 80-109 °C, which has been described to dislocation effects [20]. The dislocation population is very stable and the peak did not disappear after annealing up to 480 °C. This high stability of the internal friction peak is likely due to pinning of dislocations in the grain boundaries.

3.1. Strain hardening

Strain hardening observed at lower temperatures is due to multiplication of dislocations pinned in grain boundaries. Local maximum at the onset of the stress strain curve seems to be a consequence of the avalanche release of dislocation sources when the stress reached its critical value. At temperatures higher than 100 °C, the strain hardening rate is very low because the densities of dislocations appear to saturate due to dynamic recovery. The steady-state density of dislocations is determined by a dynamic balance between dislocation generation during plastic deformation and annihilation in the recovery process. Dislocations are generated from very close spaced sources (grain boundaries). They are close to sinks (such as grain boundaries), and interact readily so that the dislocation annihilation rates are high. Such a dynamic recovery process balances out the generation of dislocations during plastic deformation, leading to a steady-state defect density (and cell/grain size) and hence an apparent absence of strain hardening.

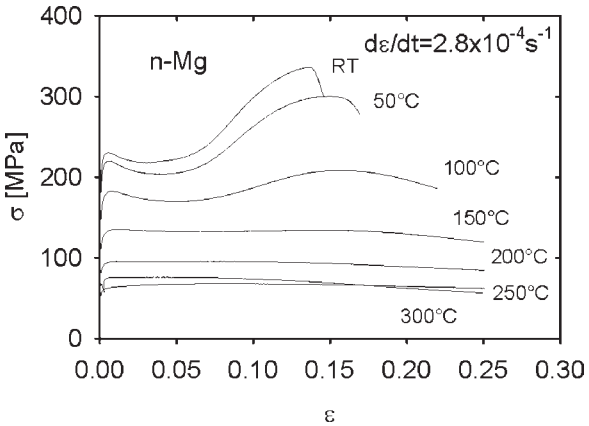

Fig. 1. Stress strain curves obtain for various temperatures.

3.2. Internal stress

Possible existence of a threshold stress, reported in [19], may be verified by the stress relaxation tests. This method allows finding thermally independent component of the applied stress.

The stress, that is necessary for dislocation motion in the slip plane, can be divided into two components

$$\tau = \tau_i + \tau^*, \tag{1}$$

where τ_i is the athermal component of the stress (internal stress) and τ^* is the temperature dependent component (effective stress). The internal stress acting on the dislocation is determined by the details of the internal structure at that moment and it is independent of the applied stress. The stress that changes when the applied stress is changed is only the effective stress. However, since the average internal stress determined microscopically is that corresponding to the average dislocation velocity, it is not guaranteed to be independent of the applied stress. In polycrystalline materials, the acting stress is related to the shear stress τ in the slip plane by the Taylor factor ψ as

$$\sigma = \psi\tau \tag{2}$$

and then similarly, it may be also divided into the internal and effective stress component:

$$\sigma = \sigma_i + \sigma^*. \tag{3}$$

Stress relaxation can be considered as a method for studying the internal stress field, based on the flow stress components separation i. e. on the determination of the average effective internal stress $(\sigma_i)_{\text{eff}}$. For the simplicity it will be called the internal stress σ_i.

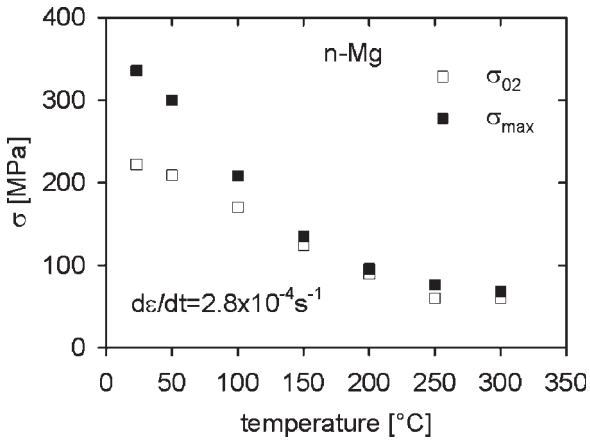

Fig. 2. Temperature dependence of the yield stress as well as the maximum stress.

3.3. Stress relaxation tests

Plastic strain of the sample during the stress relaxation test is due to a decrease of elastic strain of the deformation machine and the elastic stress of the sample itself. The stress drop rate in a stress relaxation is proportional to the plastic strain rate, i.e. $-\dot{\sigma} = C\dot{\varepsilon}$.

Considering that the stress decrease rate is proportional to the dislocation velocity *v*, it is possible to write

$$\dot{\varepsilon} = (1/\psi)\rho_m b v, \tag{4}$$

where ρ_m is the mobile dislocation density and *b* is the Burgers vector. The relation between the dislocation velocity *v* and the effective stress may be expressed by the empirical relationship proposed by Johnston and Gilman [21]:

$$v = \alpha(\sigma - \sigma_i)^m = (\sigma^*)^m. \tag{5}$$

The activation volume *V* can be defined as

$$V = kT\frac{\partial \ln v}{\partial \sigma}. \tag{6}$$

Using Eqs. (5) and (6), one can find

$$V = kT\frac{m}{\sigma - \sigma_i}. \tag{7}$$

In a stress relaxation test the stress decrease $\dot{\sigma}$ is proportional to the dislocation velocity *v*

$$\dot{\sigma} = -av, \tag{8}$$

with *a* determined by geometry, dislocation density, and modulus of elasticity. The differential equation

$$\dot{\sigma} = \alpha a(\sigma - \sigma_i)^m, \tag{9}$$

can be solved and the following relationships may be written:

$$\ln(-\dot{\sigma}) = \ln(a\alpha) + m\ln(\sigma - \sigma_i), \tag{10}$$

$$\sigma - \sigma_i = [a\alpha(m-1)]^{\frac{1}{1-m}}(t + t_0)^{\frac{1}{1-m}}, \tag{11}$$

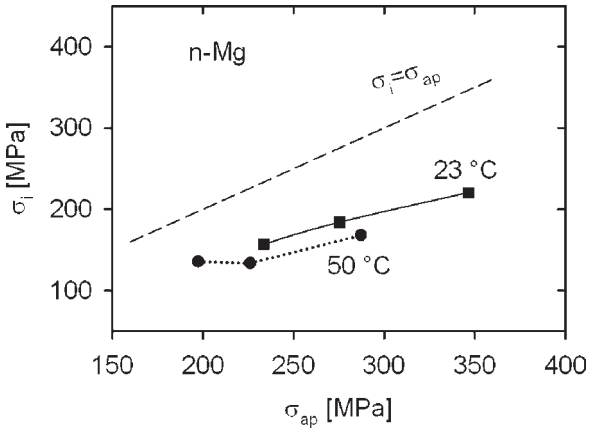

Fig. 3. Internal stress obtained at two temperatures.

$$\ln(-\dot{\sigma}) = \frac{1}{1-m}\ln(m-1) + \frac{1}{1-m}\ln(a\alpha) + \frac{m}{1-m}\ln(t+t_0), \quad (12)$$

and

$$V = \frac{mkT}{\sigma - \sigma_i}. \quad (13)$$

The internal stress σ_i was estimated using Eq. (11). The results are shown in Fig 3.

The internal stress exhibits (0.58-0.68) of the applied stress σ_{ap}. Stress sensitivity parameter m estimated from the SR test is presented in Table 1; note that this parameter (m) is the reciprocal value of $m^*=d\ln\sigma / d\ln\dot{\varepsilon}$ usually used for material characterization.

Very low values 0.004-0.04 of the strain rate sensitivity parameter are usually estimated in nc materials. Comparable values of $1/m = m^* = 0.3–1.0$, have been reported for nc Ni [8], nc Au [22], and electrodeposited Cu with predominantly nanoscale small-angle grain boundaries [23]. It should be mentioned that these values were determined in creep experiments i.e. at the low strain rates. Such values of the strain sensitivity parameter indicate deformation mechanism of Coble creep and grain boundary sliding.

The values of the apparent activation volume estimated from Eq. (13) are very small $V \sim 4\text{-}6\ b^3$ (b is the Burgers vector). In coarse grained metals, the activation volume V scales with $\sqrt{\rho}$ (considering a simple activation process such as intersection of forest dislocations and σ scales with $\sqrt{\rho}$ (where ρ is dislocation density). From Eq. (13) it follows that at a given temperature $1/m$ is approximately independent of σ and hence only very weakly dependent on the grain size d. Therefore, the relatively high value of m estimated in this study for Mg $m^*=1/m$ for linear size of ≈100 nm cannot be explained by the 'normal' activated mechanism. The measured values of V are too small for a lattice dislocation process. The 'normal' activation mechanism (such as cutting of forest dislocations in the grains interior) is likely to be replaced by the generation of dislocations from grain boundaries. Relatively large values of m = 0.14 were reported by Valiev *et al.* [24] for Cu (d = 100 nm) prepared by 16 ECAP passes. In terms of ductility, the stress–strain curve shows a total elongation to failure of >50%, and the high m may be a factor stabilizing tensile deformation. According to [25], high values of m can be found for metals with the low melting point or in materials with 'highly nonequilibrium' grain boundary structures. The consolidation route may reach such grain structures.

4. CONCLUSIONS

i) Compressive stress strain curves obtained at various temperatures exhibit a significant hardening at temperatures up to 100 °C. The stress strain curves estimated at higher temperatures have a steady state character.

Table 1. Stress sensitivity parameter estimated for two temperatures.

σ_{ap} [MPa]	m (23 °C)	m^* (23 °C)	σ_{ap} [MPa]	m (50 °C)	m^* (50 °C)
233.4	3.2	0.31	197.4	3.6	0.28
275.4	3.1	0.32	226.1	3.4	0.29
346.5	3.1	0.32	287.4	3.1	0.32

ii) Local maximum observed on curves at RT, 50 °C, and 100 °C is very probably due to avalanche multiplication of dislocations at the onset of the deformation process.

iii) Internal stress estimated from the stress relaxation tests at lower temperatures forms a substantial component of the applied stress.

iv) Relatively high values of the strain sensitivity parameter and low values of the activation volume indicate some new rate-controlling deformation mechanisms insignificant in their coarse-grained counterparts. One possibility is the emission of dislocation from boundaries, or penetration through a boundary where dislocations are concentrated locally, leading to a small activation value.

ACKNOWLEDGEMENTS

The authors are very grateful to Prof. H. Ferkel for supplying of nanocrystalline magnesium. This work is a part of the research plan MSM 0021620834 that is financed by the Ministry of Education of the Czech Republic.

REFERENCES

[1] E.O. Hall // *Proc. Phys. Soc. B* **64** (1951) 747.
[2] N.J. Petch // *Iron Steel Inst.* **174** (1953) 25.
[3] M. Mabuchi, K. Ameyama, H. Iwasaki and K. Higashi // *Acta Mater.* **46** (1999) 2024.
[4] L. Lu and L. Froyen // *Scr. Mater.* **40** (1999) 1117.
[5] L. Lu, M.O. Lai, Y.H. Toh and L. Froyen // *Mater. Sci. Eng. A* **334A** (2001) 163.
[6] J.M. Wu and Z.Z. Li // *J. Alloys Compd.* **9** (2000) 2999.
[7] S. Hwang, C. Nishimura and P.G. McCormick // *Scr. Mater.* **44** (2001) 2457.
[8] N. Wang, Z. Wang, K. T. Aust and U. Erb // *Mater. Sci. Eng. A* **237** (1997) 150.
[9] B. Cai, Q. P. Kong, L. Lu and K. Lu // *Mater. Sci. Eng. A* **286** (2000) 188.
[10] R. Z. Valiev, E. V. Kozlov, Y. F. Ivanov, J. Lian, A. A. Nazarov and B. Baudelet // *Acta Metall. Mater.* **42** (1994) 2467.
[11] A.A. Karimpoor, U. Erb, K.T. Aust and G. Palumbo // *Scripta Materialia* **49** (2003) 651.
[12] F. A. Mohamed // *Acta Materialia* **51** (2003) 4107.
[13] H. Van Swygenhoven, M. Spaczer, A. Caro and D. Farkas // *Phys. Rev. B* **60** (1999) 22.
[14] K.S. Kumar, H. Van Swygenhoven and S. Suresh // *Acta Materialia* **51** (2003) 5743.
[15] A.A. Fedorov, M.Yu. Gutkin and I.A. Ovid'ko // *Acta Materialia* **51** (2003) 887.
[16] W. W. Milligan, S. A. Hackney, M. Ke and E. C. Aifantis // *Nanostruct. Mater.* **2** (1993) 267.
[17] B. Cai, Q. P. Kong, L. Lu and K. Lu // *Mater. Sci. Eng. A* **286** (2000) 188.
[18] T. R. Malow, C. C. Koch, P. Q. Miraglia and K. L. Murty // *Mater. Sci. Eng. A* **252** (1998) 36.
[19] S. Hwang and C. Nishimura and P.G. McCormick // *Scripta mater.* **44** (2001) 1507.
[20] Z. Trojanová, B. Weidenfeller, P. Lukáč, W. Riehemann and M. Staněk, In: *Proc. of NanoSPD2, Wien, Austria, Dec9-13,2002*, ed. by M. Zehetbauer and R.Z. Valiev (J. Wiley VCH Weinheim, Germany, 2004) p. 413.
[21] W.G. Johnston and J.J. Gilman // *Solid State Phys.* **13** (1962) 147.
[22] H. Tanimoto, S. Sakai and H. Mizubayashi // *Nanostruct. Mater.* **12** (1999) 751.
[23] B. Cai, Q.P. Kong, L. Lu and K. Lu // *Script Mater.* **41** (1999) 755.
[24] R.Z. Valiev, I.V. Alexandrov, Y.T. Zhu and T.C. Lowe // *J. Mater. Res.* **17** (2002) 5.
[25] Y.M. Wang and E. Ma // *Mater. Sci. Eng. A* **375–377** (2004) 46.